Inorganic Chemistry
Cite This: Inorg. Chem. 2019, 58, 10665−10670
Article
pubs.acs.org/IC

Structural Characterization of Aurophilic Gold(I) Iodide under High Pressure

Virginia Monteseguro,*[,†] Daniel Errandonea,[†] Srungarpu N. Achary,[‡] Juan A. Sans,[§] F. Javier Manjón,[§] Samuel Gallego-Parra,[§] and Catalin Popescu[∥]

[†]Departamento de Física Aplicada-ICMUV, MALTA Consolider Team, Universitat de Valencia, Edificio de Investigación, c/Dr. Moliner 50, Burjassot, 46100 Valencia, Spain

[‡]Bhabha Atomic Research Center, Chemistry Division, Bombay 400085, Maharashtra, India

[§]Instituto de Diseño para la Fabricación y Producción Automatizada, MALTA Consolider Team, Universitat Politècnica de València, 46022 Valencia, Spain

[∥]CELLS-ALBA Synchrotron Light Facility, 08290 Cerdanyola, Barcelona, Spain

ABSTRACT: The effects of pressure on the crystal structure of aurophilic tetragonal gold iodide have been studied by means of powder X-ray diffraction up to 13.5 GPa. We found evidence of the onset of a phase transition at 1.5 GPa that is more significant from 3.8 GPa. The low- and high-pressure phases coexist up to 10.7 GPa. Beyond 10.7 GPa, an irreversible process of amorphization takes place. We determined the axial and bulk compressibility of the ambient-pressure tetragonal phase of gold iodide up to 3.3 GPa. This is extremely compressible with a bulk modulus of 18.1(8) GPa, being as soft as a rare gas, molecular solids, or organometallic compounds. Moreover, its response to pressure is anisotropic.

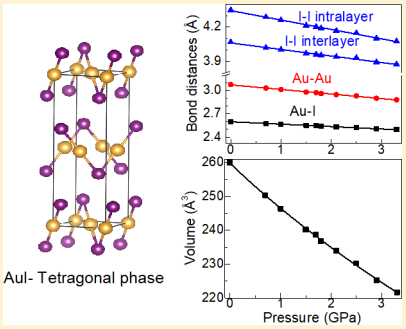

1. INTRODUCTION

The expansion of high-pressure (HP) research due to the development of diamond-anvil cells and associated characterization techniques has led to many important breakthroughs during the past decade.[1] In particular, HP could radically modify the physical and chemical properties of materials leading frequently to unexpected structural transformations.[2] This has recently driven the discovery of new materials or new phases of known materials with unique properties.[3,4] Among inorganic compounds, a vast majority of HP studies have been focused on nitrides and oxides.[3,5] In contrast with those inorganic compounds, less effort has been devoted to studying the behavior under compression of aurophilic compounds, like gold iodide (AuI).

The most important feature of AuI is the enticing interaction between closed-shell Au^+ centers. It is the general trend of metal (M) aggregates to reproduce the topology of their metallic fcc structures. Thus, M−M distances of such aggregates take values close to these observed in their metallic structures.[6] They are clearly shorter than the sum of two van der Waals radii (3.7 Å), in favorable cases as short as 2.7 Å, but generally around 3 Å.[7] This interaction is commonly termed aurophilic bonding, and in general it has a strength of 29− 46 kJ/mol, similar to that of hydrogen bonding. Such interaction gives rise to the formation of dimers, oligomers, and infinite chains.[8,9] This effect is stronger for Au than for copper (Cu) or silver (Ag) due to relativistic effects of the former. Twenty-eight percent of the binding energy in Au^+ complexes with aurophilic interactions can be attributed to relativistic expansion of the Au-d orbitals.[10] Currently, the similarity in strength between hydrogen bonding and aurophilic interaction has proven to be a convenient tool in the field of polymer and supramolecular chemistry. To date, the study of the aurophilicity under compression has been very limited.[11,12] For this reason, our HP crystallographic study will improve our understanding of the HP behavior of these aurophilic materials, i.e., as the pressure affects the Au−Au interaction that gives rise to aurophilic bonds within inorganic structures.

On the other hand, interest in the HP behavior of metal iodides has recently been stimulated by the discovery that pressure-driven structural changes can induce a giant barocaloric effect in silver iodide (AgI). Such an effect is associated with a pressure-driven decrease in the superionic transition temperature.[13] This phenomenon can be extremely useful for developing environmentally friendly cooling devices.[14,15] Such a breakthrough has shown the need for information about the influence of pressure in the crystal structures of AgI and other noble metal iodides, like AuI and copper iodide (CuI). In this context, the crystal structure of AgI has been studied up to nearly 10 GPa, and up to four different polymorphs have been reported.[16,17] The subsequent transitions transform AgI from a wurtzite to a rock-salt structure, via a zinc-blende structure, finally reaching a

Received: February 14, 2019
Published: August 7, 2019

DOI: 10.1021/acs.inorgchem.9b00433
Inorg. Chem. 2019, 58, 10665−10670

tetragonal structure in which atoms are octahedrally coordinated. In the case of CuI, several phase transitions have been found in the same pressure range.[18,19] The structural sequence goes from the zinc-blende structure to rhombohedral, tetragonal, and cubic rock-salt phases. A tetragonal post-rock-salt structure has been reported, the atoms being tetrahedrally coordinated. However, the information about HP structures provided by neutron and X-ray diffraction (XRD) experiments and theoretical calculations is contradictory.[20] Surprisingly, to date, AuI has never been studied at HP. The scarce information about AuI concerns both high-pressure and ambient conditions.

To improve our understanding of the HP structural behavior of aurophilic metal iodides, we have studied AuI up to 13.5 GPa with synchrotron-based powder XRD. Our results reveal the shortest Au−Au aurophilic distance, 2.882 Å, reported so far in inorganic solids, at a pressure of 3.3 GPa. Moreover, we have found that in contrast with AgI and CuI counterparts only one phase transition occurs in AuI up to 10.7 GPa. We have also discovered evidence of the occurrence of a pressure-induced amorphization (PIA) beyond 10.7 GPa. The compressibility of the low-pressure (LP) structure has been determined. Details of the experiments will be given in the next section, and the results will be presented and discussed in Results and Discussion.

2. EXPERIMENTAL DETAILS

For the experiments, we used 99.9% pure AuI powder from Sigma-Aldrich packed under argon. This powder contains impurities of metallic gold that give a yellow coloration. HP experiments were carried out using a membrane diamond-anvil cell (DAC) with diamond culets of 500 μm and an Inconel gasket preindented to 40 μm. To reduce the exposure to moisture and light as well as to avoid chemical reactions, AuI was loaded directly from the packing bottle into the DAC and no pressure medium was used in the experiments. This might induce nonhydrostatic conditions; however, due to the small bulk modulus of AuI [we determined it to be 18.1(8) GPa as we will explain below], deviatoric stresses can be neglected in the pressure range covered by our experiments ($P \leq 13.5$ GPa).[23,24] To determine the pressure, we used the diffraction peaks of gold impurities as the pressure standard.[25] HP angle-dispersive powder XRD measurements were carried out at room temperature at the Materials Science and Powder Diffraction beamline of ALBA Synchrotron.[26] We used a monochromatic X-ray beam (λ = 0.4642 Å) focused down to a 20 μm × 20 μm area and a Rayonix CCD detector. The sample−detector distance (210 mm) and the beam center position were calibrated using the FIT2D software[27] with the LaB_6 diffraction pattern measured under the same conditions that were used for the sample. During acquisition, the DAC was rocked by ±3° to obtain a uniform intensity distribution in the diffraction images collected at the detector. These images were integrated using DIOPTAS software[28] to analyze them using PowderCell[29] and FullProf.[30]

3. RESULTS AND DISCUSSION

Figure 1 shows the XRD pattern measured at ambient pressure in the DAC together with the Rietveld refinement. This structural refinement confirms the tetragonal crystal structure (space group $P4_2/ncm$) reported by Jagodzinski[22] as can be seen in the figure by the quality of the Rietveld fit and the small residuals. This structure has four formula units per unit cell (Z = 4). All of the peaks in the XRD pattern can be assigned either to this structure or to Au. The following ambient-condition unit-cell parameters were determined from our experiment: a = 4.355(3) Å, and c = 13.709(9) Å. The

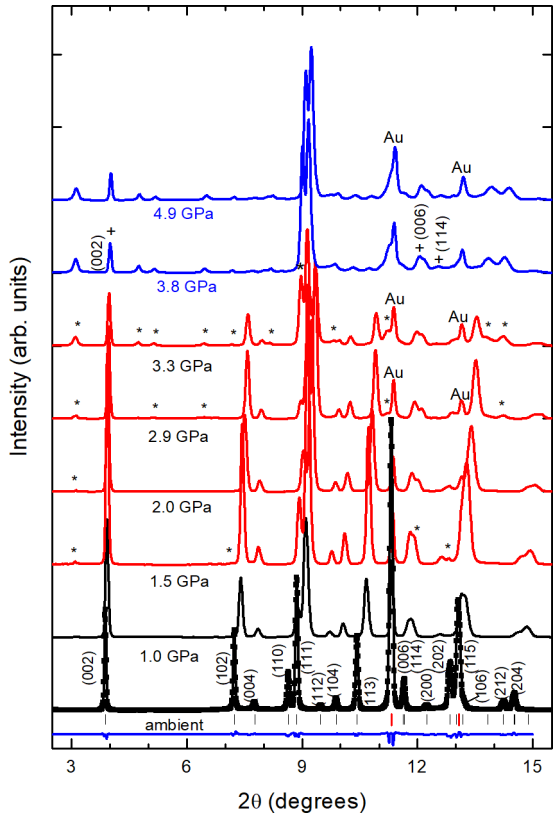

Figure 1. Selected XRD patterns of AuI measured from ambient pressure to 4.9 GPa. The patterns at the two lowest pressures (black lines) can be assigned to the LP phase. The Rietveld refinement at 0 GPa is represented. The experimental pattern is represented with black dots. The black (blue) solid line shows the refinement (residual). The black (red) ticks are positions of Bragg peaks of AuI (Au). From 1.5 to 3.3 GPa (red lines), new peaks appear, which are denoted by asterisks. Patterns at 3.8 and 4.9 GPa (blue lines) belong to the novel HP phase with the remaining contribution of the LP phase [(002), (006), and (114) Bragg reflections] labeled with a plus. The peaks from Au are signaled. In the ambient-pressure pattern, the peaks of tetragonal AuI are indexed.

following goodness-of-fit factors of the refinement were determined: R_P = 2.19%, R_{WP} = 2.83%, and χ^2 = 1.16. With regard to the atomic positions in the LP phase of AuI, Au atoms are at high-symmetry Wyckoff position 4d (0, 0, 0) and the iodine(I) atoms are at position 4e (0.25, 0.25, 0.1530 (9)), being the z coordinate of I, the only free positional parameter, which was determined from the refinement.

The crystal structure of the LP tetragonal polymorph of AuI (Figure 2a) basically consists of −I−Au−I−Au−I− polymeric zigzag chains, which form layers oriented perpendicular to the c-axis. The Au and I atoms are bonded by means of covalent bonds. Proof of that is the difference in electronegativity of the Au and I atoms. The difference is 0.12, which means that the Au−I bond is covalent with a low bond polarity. The infinite zigzag chains in the solid (Figure 2b) are linked via Au···Au aurophilic interactions along the Au plane (a−b plane) analogous to an fcc close-packing array. Notice that within each layer there is an inversion center between parallel chains and that in neighboring layers the chains run in two perpendicular directions (Figure 2c). The layers are held together along the c-axis by van der Waals forces among I atoms. At ambient pressure, the shortest interatomic distances

DOI: 10.1021/acs.inorgchem.9b00433
Inorg. Chem. 2019, 58, 10665−10670

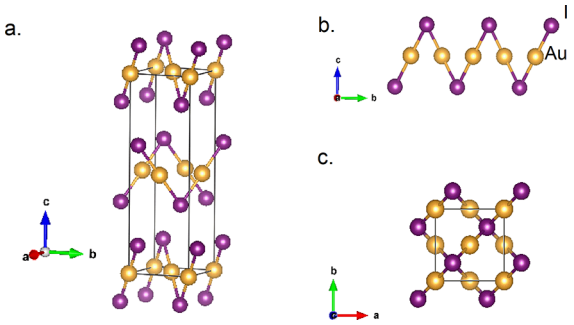

Figure 2. (a and c) Schematic views from different perspectives of the crystal structure of the LP phase of AuI. (b) Infinite chain linked via Au···Au interaction. I atoms are represented as violet spheres, and the Au atoms as yellow spheres.

are those of intralayer Au−I bonds shown in Figure 3a, which are 2.602 Å, and the Au−I−Au angle in the zigzag chains is 72.42°. Within each layer, the Au atoms form an fcc-like square two-dimensional (2D) network in which the Au−Au distance is equal to $a/\sqrt{2}$ = 3.076 Å, which is a typical distance of

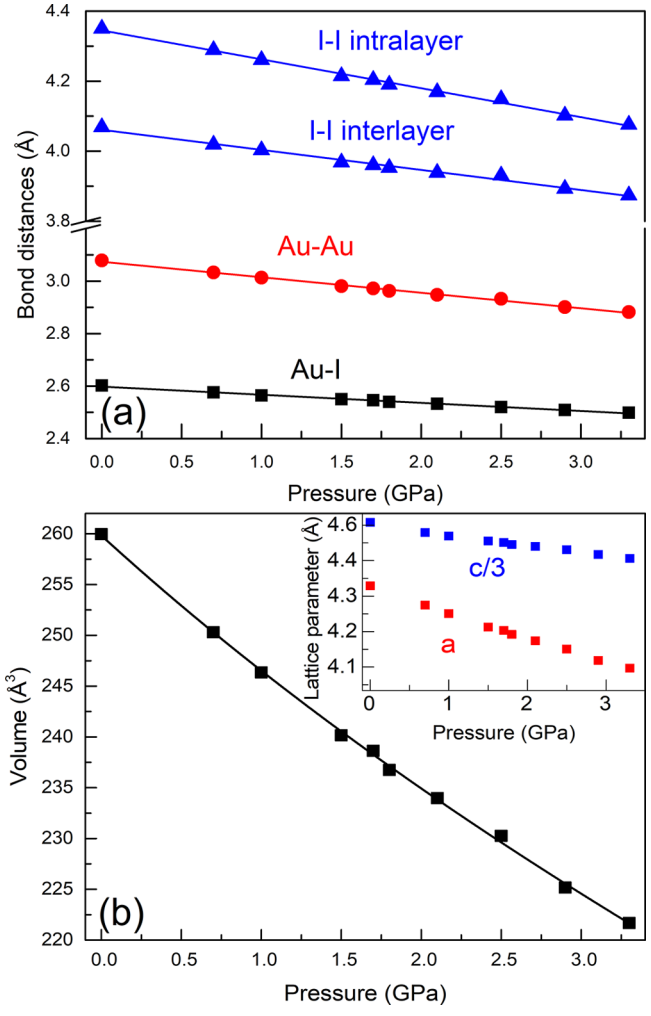

Figure 3. (a) Evolution of distances of the LP phase of AuI with pressure from 0 to 3.3 GPa. (b) Pressure dependence of the unit-cell volume of the LP phase of AuI. Black symbols (line) correspond to experimental (EOS fit) data. The inset shows the pressure dependence of the lattice parameters of the LP phase.

aurophilic bonds under ambient conditions (Figure 3a).[6,7] We can compare this Au−Au distance with those of other aurophilic structures, e.g., in gold chloride AuCl,[31] 3.22 Å, in organometallic solids like [1,4-C_6H_4{PPh_2(AuCl)}$_2$], 3.6686(5) Å, and in $AuEt_2DTC{\cdot}xCH_2Cl_2$, 2.78 Å.[11,12] The Au−Au distance in AuI is significantly shorter than in two of these reported above. On one hand, I atoms in each layer form simple square 2D networks at each side of the Au network in which the distance between I atoms is equal to the unit-cell parameter *a*, i.e., 4.355(3) Å. On the other hand, I atoms from subsequent layers are arranged in such a way that they make a regular square pyramid, where one I atom at one layer (the vertex of the pyramid) is separated from the other four I atoms in the neighboring layer (the base of the pyramid) by 4.069(3) Å (Figure 3a). The tetragonal phase of AuI retains the square lattice of fcc-Au, but with expanded Au−Au distances due to the incorporation of I atoms in the structure of Au metal. Recently, a close-packing array of Sn atoms, like those present in pure fcc-Sn, has been found in $CaCl_2$-type SnO_2. This supports the argument that the cation array is the major factor governing structure formation and evolution under pressure.[32] These examples cannot be a mere coincidence and seem to provide support for the "anions in metallic matrices" model.[33]

Figure 1 shows XRD patterns obtained under compressions of ≤4.9 GPa. As the pressure increases, the typical shift of peaks toward higher angles due to the reduction of unit-cell parameters is observed. It is interesting that the (102) peak shifts faster than the (002) and (004) peaks, thus indicating that the compression of the crystal is anisotropic. Indeed, the (102) peak gradually approaches the (004) peak as one can see in the figure. At 1.5 GPa, a few new peaks can be detected. They are identified with asterisks in the figure. These peaks are the evidence of the onset of a structural phase transition. As the pressure increases, these peaks of the new phase, which will hereafter be denoted by the HP phase, become more intense. However, the (002), (006), and (114) Bragg reflections associated with the LP phase remain in the whole pressure range studied, which indicates the coexistence of both phases up to the amorphization. It is important to remark that the main phase from 3.8 GPa is the HP phase, because the only remaining reflections of the LP phase are those mentioned above, which gradually become weaker. For this reason, the tetragonal phase has been quantitatively analyzed under a pressure of ≤3.3 GPa, being the last pressure point at which the LP phase is the main one.

The evolution of bond distances (d) of the LP with pressure is represented in Figure 3a. Such distances were calculated through the atomic positions obtained by Rietveld refinement, being the z coordinate of I atoms, the only atomic coordinate in the fitting. The bond compressibility, defined by $\chi = -(1/d)(\partial d/\partial P)$, has been calculated for every bond in the structure and is represented in Table 1. Moreover, their pressure coefficients ($\partial d/\partial P$) are also listed. The Au−Au and I−I (intralayer) distances are the most affected by pressure with a compressibility of 2×10^{-2} GPa^{-1} in both cases. At 3.3 GPa, the Au−I distance has been reduced from the ambient pressure value (2.602 Å) to 2.499 Å (Figure 3a). On the other hand, the intralayer and interlayer I−I distances have been compressed from 4.350 and 4.069 Å to 4.076 and 3.874 Å, respectively (Figure 3a). Interestingly, at 3.3 GPa, the Au−Au distance is 2.882 Å (Figure 4a). To the best of our knowledge, this is the shortest pressure-induced Au−Au aurophilic distance in an inorganic structure and the largest pressure-induced contrac-

DOI: 10.1021/acs.inorgchem.9b00433
Inorg. Chem. 2019, 58, 10665−10670

Table 1. Bond Compressibility and Pressure Coefficients of the Au−I, Au−Au, and I−I Bonds

bond	bond compressibility ($\times 10^{-2}$ GPa^{-1})	pressure coefficient ($\times 10^{-2}$ Å/GPa)
Au−I	1.3 ± 0.3	3.1 ± 0.1
Au−Au	2.0 ± 0.3	5.9 ± 0.1
I−I (intralayer)	2.0 ± 0.3	8.3 ± 0.2
I−I (interlayer)	1.5 ± 0.2	5.7 ± 0.2

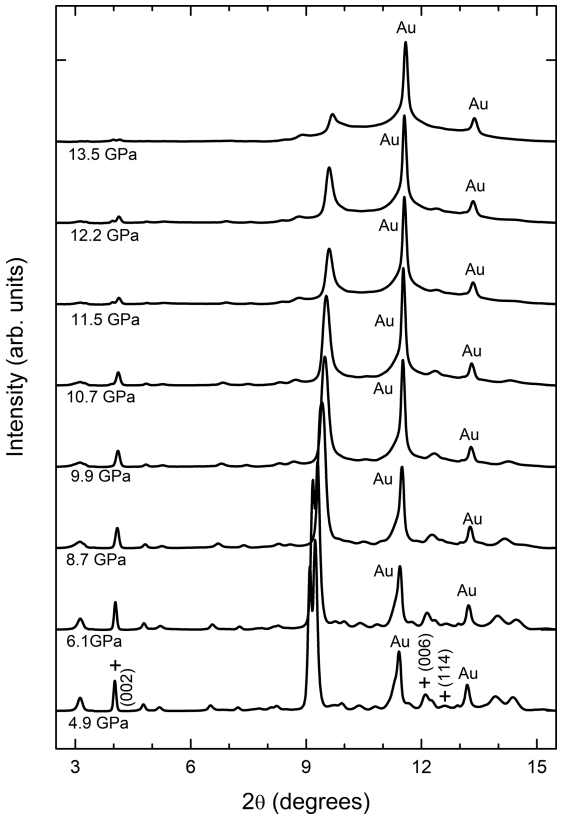

Figure 4. Selected XRD patterns of AuI measured from 4.9 to 13.5 GPa. All patterns can be assigned to the HP phase with the remaining (002) Bragg reflection of the LP phase (marked by plus). Pressures are indicated in the figure, and the peaks from Au are labeled.

tion in the length, around 0.2 Å, of an aurophilic interaction within just 3.3 GPa. Paliwoda et al. reported the pressure-induced shortening of aurophilic contacts, from 2.78 to 2.72 Å, in the organometallic gold(I) diethyldithiocarbamate polymer (organometallic solid) between 0 and 1 GPa, and O'Connor et al. published the largest pressure-induced contraction in the length of an aurophilic interaction, 0.613 Å, obtained from 0 to 10.6 GPa in another organometallic compound, [1,4-$C_6H_4\{PPh_2(AuCl)\}_2$].[11,12] If we do an extrapolation at 10.7 GPa, by using the pressure coefficient of the Au−Au distance (−0.059 Å/GPa), a length contraction of 0.63 Å is calculated, a value that is similar to that obtained by O'Connor et al. in the same pressure range for an organometallic compound.

On the other hand, from our experiments, we have obtained the pressure dependence of the unit-cell parameters of the LP phase of AuI (Figure 3b) up to 3.3 GPa. The pressure dependence for unit-cell parameters is nearly linear, but the compressibility is anisotropic, the *c*-axis being the less compressible one. The axial compressibility at ambient pressure in the different crystallographic directions, $k_x = -(1/x)\partial x/\partial P$, yield a k_a of 1.98×10^{-2} GPa^{-1} and a k_c of 9.76×10^{-3} GPa^{-1}. Because $k_a \cong 2k_c$, the tetragonal AuI is more compressible along the layers than in the direction perpendicular to the layers. This behavior is expected because the contribution of the Au−I covalent bond is stronger along the *c*-axis than in the *a*−*b* plane. In fact, the bond compressibility previously gave us an idea of how the structure is affected by pressure. The more compressible bonds are those associated with Au−Au aurophilic bonds and I−I (intralayer) bonds located in the *a*−*b* plane. From the axial compressibilities, the bulk modulus (B_0) can be determined with the equation $B_0 = 1/(2k_a + k_c)$, its value being 20 GPa. In Figure 3b, we represent the pressure dependence of the unit-cell volume of the LP phase. We have found that the pressure dependence of the unit-cell volume can be properly reproduced by a third-order Birch−Murnaghan EOS.[34,35] We have determined the unit-cell volume at ambient pressure (V_0), the bulk modulus (B_0), and its pressure derivative (B_0'). Their values are 259.8(5) Å^3, 18.1(8) GPa, and 2.0(4), respectively. The fitted EOS is shown in Figure 3b. The maximum deviation between the experimental pressure and that determined from the EOS is only 0.1 GPa, which indicates that the obtained EOS has an excellent predictive capability. Notice that the bulk modulus is similar to that determined from the linear compressibility, indicating that most of the compression of the structure occurs along the layers. In addition, B_0 is very small, comparable to that of rare-gas solids[36] and molecular solids,[23] and 50% smaller than the bulk modulus of the different polymorphs of AgI and CuI.[37−39] On the other hand, this B_0 is on the same order of magnitude as that of the aurophilic organometallic solid [1,4-$C_6H_4\{PPh_2(AuCl)\}_2$], which is 8(13) GPa.[11] Moreover, the pressure derivative of the bulk modulus is much smaller than the typical value for this parameter, which is expected to be near 4 in ionic−covalent solids.[40] Curiously, the pressure derivative in many highly compressible molecular solids and open framework structures based on van der Waals interatomic bonds is usually much higher than 4,[23,41,42] thus reflecting a large increase of the strength of van der Waals interactions with an increase in pressure. Therefore, the small value of the pressure derivative of AuI could be ascribed to the soft nature of Au−Au and I−I bonds (see Table 1). In summary, both the I−I van der Waals interactions and the Au−Au aurophilic interactions make the 2D polymeric polymorph of AuI an unusually highly compressible solid.[43,44]

Regrettably, the HP phase cannot be determined due to the quality of XRD patterns, which were spotty in spite of the 6° rocking used in the experiments, and due to the coexistence of phases. Moreover, it is worth taking into account, on one hand, the fact that a better crystallinity of the sample cannot be achieved by warming the sample because it would likely decompose or melt (melting temperature of 120 °C), which happens with other gold halide compounds. On the other hand, unfortunately, this structure cannot be confirmed by density functional theory (DFT) calculations, for the moment, due to the challenges of overcoming the tendency of gold (Au) not to form stable bonds with any atomic element in crystalline solids. According to Santamaría-Pérez et al.,[45] the DFT methods fail quite spectacularly to describe a gold compound, with 20% and 400% errors in the equilibrium volume and bulk modulus, respectively. This is due to the poor treatment of static correlation in common DFT approximations. Moreover,

DOI: 10.1021/acs.inorgchem.9b00433
Inorg. Chem. 2019, 58, 10665−10670

it is convenient to mention that DFT cannot explain the low-symmetry crystal structure of AuI (LP phase). The calculations predict zinc-blend or rock-salt structures[21] (like those found in AgI and CuI, respectively) instead of the polymeric crystal structure of AuI obtained experimentally.[22]

Upon further compression, we found the remaining LP phase and the HP phase stable up to 10.7 GPa. In Figure 4, we show XRD patterns measured from 4.9 to 13.5 GPa. There, it can be seen that the most relevant change from 4.9 to 10.7 GPa is the gradual shift of Bragg reflections toward higher angles due to a decrease in the *d* spacing as a consequence of the compression of the unit cell. At 9.9 and 10.7 GPa, a broadening of the peaks is observed probably due to nonhydrostatic effects (remember that no pressure medium is used). Beyond 10.7 GPa, we observed the XRD peaks further broaden and the intensities of them diminish, many of them disappearing. Such a phenomenon is enhanced with pressure. Moreover, it is accompanied by an increase in the background in the 9−13° region. Indeed, at 13.5 GPa, the XRD pattern basically consists of only the two Au peaks and two additional broad bands located near 9−10°. Interestingly, this process is irreversible and resembles a PIA.[46,47] The occurrence of such a phenomenon is not surprising given the similarities of the large ionic radii of Au^+ and I^-. This fact will potentially make it difficult for AuI to accommodate stresses through atomic displacements, resulting in a loss of periodicity at HP that triggers the transformation into a frustrated noncrystalline amorphous.[48,49] The broad bands near 9−10° in the XRD patterns of amorphous AuI correspond to distances of 2.75 and 3.00 Å. They can be associated with interatomic distances in the disordered phase. The causes of disordering can be mechanical or vibrational instabilities (from the material itself or caused by the nonhydrostatic nature) or even the presence of large kinetic barriers blocking the transition to a second crystalline HP phase.[50] Future studies are needed to clarify the mechanism behind pressure-induced amorphization of AuI. A possible technique could be X-ray absorption at the Au L_3 edge, 11.919 keV. Raman studies are excluded because AuI is highly photosensitive and decomposes under light, taking a dark-red color.

4. CONCLUSIONS

We have performed a high-pressure study of the structural properties of AuI up to 13.5 GPa. The crystal structures at different pressures have been determined using a diamond-anvil cell and synchrotron powder X-ray diffraction. We have rigorously studied the effects of compression in the crystal structure, finding the existence of a phase transition at 3.8 GPa (the onset being at 1.5 GPa) followed by a disordering at 11.5 GPa. In addition, we have obtained information on the axial and bulk compressibility of the LP phases of AuI. From these results, the room-temperature EOS has been obtained for this phase. The LP phase is extremely compressible, being as soft as a rare gas, a molecular solid, or an organometallic compound. Moreover, we report the shortest Au−Au aurophilic distance, 2.882 Å at 3.3 GPa, and the largest pressure-induced contraction in the length of an aurophilic interaction, 0.2 Å, in the pressure range from 0 to 3.3 GPa in an inorganic Au^+ complex. The obtained information about the high-pressure behavior of the crystal structure is useful for gaining valuable microscopic insights into the superionic features of noble metal iodides, required to improve our understanding of the barocaloric properties of these compounds, which are governed by pressure-driven structural phase transitions involving large entropy changes related to the displacement of iodine ions.[51,52]

AUTHOR INFORMATION

Corresponding Author

*E-mail: virginia.monteseguro@uv.es.

ORCID

Virginia Monteseguro: 0000-0003-2709-3879
Daniel Errandonea: 0000-0003-0189-4221
Srungarpu N. Achary: 0000-0002-2103-1063
F. Javier Manjón: 0000-0002-3926-1705

Notes

The authors declare no competing financial interest.

ACKNOWLEDGMENTS

The authors are thankful for the financial support of the Spanish Ministerio de Ciencia, Innovación y Universidades, the Spanish Research Agency (AEI), and the European Fund for Regional Development (FEDER) under Grant MAT2016-75586-C4-1/2-P and of Generalitat Valenciana under Grant Prometeo/2018/123 (EFIMAT). J.A.S. acknowledges the "Ramón y Cajal" fellowship program (RYC-2015-17482) and Spanish Mineco Project FIS2017-83295-P. V.M. acknowledges the "Juan de la Cierva" program (FJCI-2016-27921) for financial support. Experiments were performed at the Materials Science and Powder Diffraction beamline of ALBA Synchrotron. The authors are thankful for the collaboration of ALBA staff and also thank D. Santamaría-Pérez for fruitful discussions.

REFERENCES

(1) Mao, H.-K.; Chen, X.-Y.; Ding, Y.; Li, B.; Wang, L. Solids, liquids, and gases under high pressure. *Rev. Mod. Phys.* **2018**, *90*, 015007−015061.

(2) Benmakhlouf, A.; Errandonea, D.; Bouchenafa, M.; Maabed, S.; Bouhemadou, A.; Bentabet, A. New pressure-induced polymorphic transitions of anhydrous magnesium sulfate. *Dalton Trans.* **2017**, *46*, 5058−5068.

(3) Horvath-Bordon, E.; Riedel, R.; Zerr, A.; McMillan, P. F.; Auffermann, G.; Prots, Y.; Bronger, W.; Kniep, R.; Kroll, P. High-pressure chemistry of nitride-based materials. *Chem. Soc. Rev.* **2006**, *35*, 987−1014.

(4) Errandonea, D.; Garg, A. B. Recent progress on the characterization of the high-pressure behaviour of AVO4 orthovanadates. *Prog. Mater. Sci.* **2018**, *97*, 123−169.

(5) Manjon, F. J.; Errandonea, D. Pressure-induced structural phase transitions in materials and earth sciences. *Phys. Status Solidi B* **2009**, *246*, 9−31.

(6) Vegas, A. Cations in Inorganic Solids. *Crystallogr. Rev.* **2000**, *7* (3), 189−283.

(7) Schmidbaur, H. The aurophilicity phenomenon: A decade of experimental findings, theoretical concepts and emerging applications. *Gold Bulletin* **2000**, *33*, 3−10.

(8) Bachman, R. E.; Fioritto, M. S.; Fetics, S. K.; Cocker, M. T. The Structural and Functional Equivalence of Aurophilic and Hydrogen Bonding: Evidence for the First Examples of Rotator Phases Induced by Aurophilic Bonding. *J. Am. Chem. Soc.* **2001**, *123*, 5376−5377.

(9) Pyykkö, P. Strong Closed-Shell Interactions in Inorganic Chemistry. *Chem. Rev.* **1997**, *97*, 597−636.

(10) Runeberg, N.; Schütz, M.; Werner, H.-J. The aurophilic attraction as interpreted by local correlation methods. *J. Chem. Phys.* **1999**, *110*, 7210−7215.

(11) O'Connor, A. E.; Mirzadeh, N.; Bhargava, S. K.; Easun, T. L.; Schröder, M.; Blake, A. J. Aurophilicity under pressure: a combined

DOI: 10.1021/acs.inorgchem.9b00433
Inorg. Chem. 2019, 58, 10665−10670

crystallographic and in situ spectroscopic study. *Chem. Commun.* **2016**, *52*, 6769−6772.
(12) Paliwoda, D.; Wawrzyniak, P.; Katrusiak, A. Unwinding $Au^{+}\cdots Au^{+}$ Bonded Filaments in Ligand-Supported Gold(I) Polymer under Pressure. *J. Phys. Chem. Lett.* **2014**, *5*, 2182−2188.
(13) Cazorla, C.; Errandonea, D. Giant Mechanocaloric Effects in Fluorite-Structured Superionic Materials. *Nano Lett.* **2016**, *16*, 3124−3129.
(14) Aznar, A.; Lloveras, P.; Romanini, M.; Barrio, M.; Tamarit, J. L.; Cazorla, C.; Errandonea, D.; Mathur, N. D.; Planes, A.; Moya, X.; Mañosa, L. Giant barocaloric effects over a wide temperature range in superionic conductor AgI. *Nat. Commun.* **2017**, *8*, 1851−1856.
(15) Sagotra, A. K.; Errandonea, D.; Cazorla, C. Mechanocaloric effects in superionic thin films from atomistic simulations. *Nat. Commun.* **2017**, *8*, 963−969.
(16) Keen, D. A.; Hull, S.; Hayes, W.; Gardner, N. J. Structural Evidence for a Fast-Ion Transition in the High-Pressure Rocksalt Phase of Silver Iodide. *Phys. Rev. Lett.* **1996**, *77*, 4914−4917.
(17) Ohtaka, O.; Takebe, H.; Yoshiasa, A.; Fukui, H.; Katayama, Y. Phase relations of AgI under high pressure and high temperature. *Solid State Commun.* **2002**, *123*, 213−216.
(18) Hull, S.; Keen, D. A. High-pressure polymorphism of the copper(I) halides: A neutron-diffraction study to ∼ 10 GPa. *Phys. Rev. B: Condens. Matter Mater. Phys.* **1994**, *50*, 5868−5885.
(19) Blacha, A.; Christensen, N. E.; Cardona, M. Electronic structure of the high-pressure modifications of CuCl, CuBr, and CuI. *Phys. Rev. B: Condens. Matter Mater. Phys.* **1986**, *33*, 2413−2421.
(20) Zhu, J.; Pandey, R.; Gu, M. J. The phase transition and elastic and optical properties of polymorphs of CuI. *J. Phys.: Condens. Matter* **2012**, *24*, 475503−475510.
(21) Söhnel, T.; Hermann, H.; Schwerdtfeger, P. J. Solid state density functional calculations for the group 11 monohalides. *J. Phys. Chem. B* **2005**, *109*, 526−531.
(22) Jagodzinski, H. Die Kristallstruktur des AuJ. *Zeitschrift für Kristallographie* **1959**, *112*, 80−87.
(23) Sans, J. A.; Manjón, F. J.; Popescu, C.; Muñoz, A.; Rodríguez-Hernández, P.; Jordá, J. L.; Rey, F. J. Arsenolite: a quasi-hydrostatic solid pressure-transmitting medium. *J. Phys.: Condens. Matter* **2016**, *28*, 475403−475409.
(24) Errandonea, D.; Muñoz, A.; Gonzalez-Platas, J. High-pressure x-ray diffraction study of YBO_3/Eu^{3+}, $GdBO_3$, and $EuBO_3$: Pressure-induced amorphization in $GdBO_3$. *J. Appl. Phys.* **2014**, *115*, 216101−216103.
(25) Hirose, K.; Sata, N.; Komabayashi, T.; Ohishi, Y. Simultaneous volume measurements of Au and MgO to 140 GPa and thermal equation of state of Au based on the MgO pressure scale. *Phys. Earth Planet. Inter.* **2008**, *167*, 149−154.
(26) Fauth, F.; Peral, I.; Popescu, C.; Knapp, M. The new Material Science Powder Diffraction beamline at ALBA Synchrotron. *Powder Diffr.* **2013**, *28*, S360−S370.
(27) Hammersley, A. P.; Svensson, S. O.; Hanfland, M.; Fitch, A. N.; Häusermann, D. Two-dimensional detector software: From real detector to idealized image or two-theta scan. *High Pressure Res.* **1996**, *14*, 235−248.
(28) Prescher, C.; Prakapenka, V. B. DIOPTAS: a program for reduction of two-dimensional X-ray diffraction data and data exploration. *High Pressure Res.* **2015**, *35*, 223−230.
(29) Kraus, W.; Nolze, G. J. POWDER CELL - a program for the representation and manipulation of crystal structures and calculation of the resulting X-ray powder patterns. *J. Appl. Crystallogr.* **1996**, *29*, 301−303.
(30) Rodrıguez-Carvajal, J. Recent advances in magnetic structure determination by neutron powder diffraction. *Phys. B* **1993**, *192*, 55−69.
(31) Doll, K.; Pyykkö, P.; Stoll, H. Closed-shell interaction in silver and gold chlorides. *J. Chem. Phys.* **1998**, *109*, 2339−2345.
(32) Girao, H. T.; Hermet, P.; Masenelli, B.; Haines, J.; Mélinon, P.; Machon, D. Pressure-Induced Sublattice Disordering in SnO_2: Invasive Selective Percolation. *Phys. Rev. Lett.* **2018**, *120*, 265702−265707.
(33) Vegas, A.; Santamaría-Pérez, D.; Marqués, M.; Florez, M.; García Baonza, V.; Recio, J. M. Anions in metallic matrices model: application to the aluminium crystal chemistry. *Acta Crystallogr., Sect. B: Struct. Sci.* **2006**, *62*, 220−227.
(34) Birch, F. Finite strain isotherm and velocities for single-crystal and polycrystalline NaCl at high pressures and 300K. *J. Geophys. Res.* **1978**, *83*, 1257−1268.
(35) Angel, R. J. Equations of State. *Rev. Mineral. Geochem.* **2000**, *41*, 35−59.
(36) Errandonea, D.; Boehler, R.; Japel, S.; Mezouar, M.; Benedetti, L. R. Structural transformation of compressed solid Ar: An x-ray diffraction study to 114 GPa. *Phys. Rev. B: Condens. Matter Mater. Phys.* **2006**, *73*, 092106−092109.
(37) Hull, S.; Keen, D. A. Pressure-induced phase transitions in AgCl, AgBr, and AgI. *Phys. Rev. B: Condens. Matter Mater. Phys.* **1999**, *59*, 750−761.
(38) Singh, R. K.; Gupta, D. C. Phase transition and high-pressure elastic behavior of copper halides. *Phys. Rev. B: Condens. Matter Mater. Phys.* **1989**, *40*, 11278−11283.
(39) Gupta, D. C.; Singh, R. K. Pressure-induced phase transitions in silver halides. *Phys. Rev. B: Condens. Matter Mater. Phys.* **1991**, *43*, 11185−11189.
(40) Hofmeister, A. M. Pressure derivatives of the bulk modulus. *J. Geophys. Res.* **1991**, *96*, 21893−21907.
(41) Xu, M.; Jakobs, S.; Mazzarello, R.; Cho, J.-Y.; Yang, Z.; Hollermann, H.; Shang, D.; Miao, X. S.; Yu, Z. H.; Wang, L.; Wuttig, M. Impact of Pressure on the Resonant Bonding in Chalcogenides. *J. Phys. Chem. C* **2017**, *121*, 25447−25454.
(42) Pereira, A. L. J.; Sans, J. A.; Vilaplana, R.; Gomis, O.; Manjón, F. J.; Rodríguez-Hernández, P.; Muñoz, A.; Popescu, C.; Beltrán, A. Isostructural Second-Order Phase Transition of β-Bi_2O_3 at High Pressures: An Experimental and Theoretical Study. *J. Phys. Chem. C* **2014**, *118*, 23189−23201.
(43) Boultif, A.; Louër, D. J. Powder pattern indexing with the dichotomy method. *J. Appl. Crystallogr.* **1991**, *24*, 987−993.
(44) Errandonea, D. Exploring the properties of MTO_4 compounds using high-pressure powder x-ray diffraction. *Cryst. Res. Technol.* **2015**, *50*, 729−736.
(45) Santamaría-Pérez, D.; Daisenberger, D.; Ruiz-Fuertes, J.; Marqueño, T.; Chulia-Jordan, R.; Muehle, C.; Jansen, M.; Rodriguez-Hernandez, P.; Muñoz, A.; Johnson, E. R.; Otero-de-la-Roza, O. Gold(I) sulfide: unusual bonding and an unexpected computational challenge in a simple solid. *Chem. Sci.* **2019**, *10*, 6467−6475.
(46) Pereira, A. L. J.; Errandonea, D.; Beltran, A.; Gracia, L.; Gomis, O.; Sans, J. A.; Garcıa-Domene, B.; Miquel-Veyrat, A.; Manjon, F. J.; Muñoz, A.; Popescu, C. Structural study of α-Bi2O3 under pressure. *J. Phys.: Condens. Matter* **2013**, *25*, 475402−475413.
(47) Arora, A. K.; Sato, T.; Okada, T.; Yagi, T. High-pressure amorphous phase of vanadium pentaoxide. *Phys. Rev. B: Condens. Matter Mater. Phys.* **2012**, *85*, 094113−094120.
(48) Serghiou, G.; Reichmann, H. J.; Boehler, R. Size criterion for amorphization of molecular ionic solids. *Phys. Rev. B: Condens. Matter Mater. Phys.* **1997**, *55*, 14765−14769.
(49) Errandonea, D.; Somayazulu, M.; Häusermann, D. Phase transitions and amorphization of $CaWO_4$ at high pressure. *Phys. Status Solidi B* **2003**, *235*, 162−169.
(50) Mao, H.-K.; Chen, B.; Chen, J.; Li, K.; Lin, J.-F.; Yang, W.; Zheng, H. Recent advances in high-pressure science and technology. *Matter and Radiation at Extremes* **2016**, *1*, 59−75.
(51) Bermúdez-García, J. M.; Sánchez-Andújar, M.; Señarís-Rodríguez, M. A. A New Playground for Organic−Inorganic Hybrids: Barocaloric Materials for Pressure-Induced Solid-State Cooling. *J. Phys. Chem. Lett.* **2017**, *8*, 4419−4423.
(52) Cazorla, C.; Sagotra, A. K.; King, M.; Errandonea, D. High-Pressure Phase Diagram and Superionicity of Alkaline Earth Metal Difluorides. *J. Phys. Chem. C* **2018**, *122*, 1267−1279.

DOI: 10.1021/acs.inorgchem.9b00433
Inorg. Chem. 2019, 58, 10665−10670